Clemente-Castro *et al.*
Environmental Sciences Europe (2023) 35:88
https://doi.org/10.1186/s12302-023-00800-w

Environmental Sciences Europe

RESEARCH

Open Access

Optimizing pyrolysis parameters and product analysis of a fluidized bed pilot plant for *Leucaena leucocephala* biomass

S. Clemente-Castro[1], A. Palma[1*], M. Ruiz-Montoya[1], I. Giráldez[2] and M. J. Díaz[1]

Abstract

This study aimed to optimize the production of bio-oil from *Leucaena leucocephala* wood using a fluidized bed reactor. Response surface methodology was used to optimize the fast pyrolysis through three operational parameters: pyrolysis temperature, nitrogen flow rate, and temperature of the first condensation stage. The optimum conditions obtained for bio-oil production were 500 °C, 26.4 L min^{-1}, that is, about 3.3 times the minimum fluidization flow, and 80 °C, respectively. The bio-oil obtained under optimum conditions was of good quality and did not require further treatment. Physical properties of the bio-oil were analysed according to ASTM D7544-12. In addition, the chemical composition of the non-condensed gases and bio-oil were identified using GC–MS. The non-condensed gases were found to contain mainly ketones and lignin derivatives, while the bio-oil contained cyclic ketones, alcohol ethers, aromatic alcohols, and lignin derivatives. The study found that increasing the pyrolysis temperature did not significantly increase the yield of H_2 and CO for syngas production. Regarding the solid obtained, a large amount of unreacted material (66.7 wt.%) is generated at 400 °C, and as the temperature is increased, a high-quality biochar is obtained.

Keywords Leguminous, Biofuel, Pyrolysis, Bio-oil, Biochar, Hydrogen

Introduction

Given the new perspectives in environmental issues and the constant search for alternatives to improve energy processes, biomass is postulated as one of the keys to production of clean and safe energy. Pyrolysis, which produces liquids (bio-oil), solid (biochar) and gases with a certain content of syngas (H_2+CO), is one of the thermochemical treatments that makes the best use of the biomass produced [1]. This process, which destroys the lignocellulosic biomass structure at high temperatures in the absence of an oxidizing agent, produces a liquid that can be assimilated into a liquid fuel called bio-oil, with a composition based mainly on carbonyl, phenolic and carboxylic groups [2]. Some of the most recent reports on the cost of bio-oil production using lignocellulosic biomass pyrolysis technologies estimate it at 0.353 $/L or 9.56 $/GJ, others are more optimistic at 0.206 $/L or 9.57 $/GJ, but in general and comparing everything, it indicates that the production costs of bio-oil is moderate [3, 4]. Despite the advantages of pyrolysis to produce bio-oil, this product obtained from lignocellulosic biomass has very poor characteristics for direct use in existing combustion and utilization equipment due to its high oxygen and moisture content, high viscosity and acidity, as well as low stability and low calorific value [5], compared to, for example, bio-oil obtained by pyrolysis of triglycerides [6]. Therefore, the search for the best working conditions in lignocellulosic biomass pyrolysis and the

*Correspondence:
A. Palma
alberto.palma@diq.uhu.es
[1] Department of Chemical Engineering, Physical Chemistry and Materials Science, University of Huelva, Campus "El Carmen", 21071 Huelva, Spain
[2] Department of Chemistry "Prof. José Carlos Vílchez Martín", University of Huelva, Campus "El Carmen", 21071 Huelva, Spain

most suitable pretreatment is crucial for the implementation of the process. The adaptation of the raw material enough so that the bio-oil meets the existing quality standards in the legislation is a step of due compliance, low humidity level, high calorific value with adequate stability, are just some of the most widespread prerogatives to use bio-oil in commercial burners and that they manage to adapt to the two ASTM and CEN standards as the most representative [7].

Lignocellulosic biomass is divided into three main compounds: hemicellulose, cellulose and lignin, each of which are distributed and combined in very different ways depending on its species and origin. During the lignocellulosic biomass degradation process, hemicellulose, the component most susceptible to volatilization, is mainly converted into furans, anhydrosugars, and light oxygenated compounds that could produce bio-oil [8]. Cellulose, although it does not differ much from hemicellulose in terms of its destructive capacity in the temperature range, is present in more abundance and produces many more volatile sugars and light compounds that will form the basis of the bio-oil in the pyrolysis of lignocellulosic materials [8, 9]. As for lignin, it is known that it tends to produce biochar solid, although a certain amount manages to transform into condensable light aromatic compounds, typically phenolic molecules, which will be part of the bio-oil at moderately high temperatures [10].

One of the most promising lignocellulosic species is leguminous biomass, whose nitrogen fixation properties and versatility of its applications make it very interesting as an alternative to traditional fast-growing energy crops [11]. In particular, attention has been drawn in recent years to *Leucaena leucocephala*, a fast-growing shrub or even tree with a high capacity to adapt to both wet and dry climates and with very favourable reforestation rates and contaminated soils treatment [12]. This specific legume species will be the one to be explored in this study by means of pyrolysis treatment to verify its viability and the possible potential applications of its products and residues. The viability of this raw material is developing and studies on its implementation in increasingly arid climates such as the Mediterranean are highly appreciated, giving *L. leucocephala* a good perspective for the future with regard to its implementation at the biorefinery level [13].

Pyrolysis technologies can be divided into two categories: slow and fast, based on the heating time of the fuel up to the pyrolysis temperature and the reaction time. In slow pyrolysis, the residence time is of the order of minutes or more and the main objective is to produce a solid char. However, fast pyrolysis occurs with very short vapour residence times (seconds or even milliseconds), producing liquid and gas, and it is further subdivided into flash and ultrarapid pyrolysis [14]. To promote the formation of high-quality bio-oil and gas, the configuration of the pyrolysis reactors is crucial. There are many types of reactors such as fixed bed reactor, fluidized bed reactor (subdivided into bubbling, circulating and spouted), ablative, vacuum, rotating cone and auger reactor [15]. Although all of these techniques have great potential for liquid production, some of them require very specific control and are still under development. Fluidized bed reactors are the ones that have received the most attention from researchers due to their proven ability to produce high-quality bio-oil due to the excellent surface contact between the biomass and the bed under fluidization conditions [16]. Auger reactors are the other technology that has taken over the pyrolysis process, in this case at the level of small-to-medium scale industrial plants for the treatment of lignocellulosic, plastic, and municipal and industrial solid waste. In this reactor configuration, the material is fed into a cylindrical tube without an oxidizing agent, allowing the gas residence time to be controlled by varying the heated area. Some of the features that have led to consideration by industry and science are ease of scaling and flexibility of operation and feedstock [17, 18].

Fluidization technology, in both in bubbling and circulating reactors, is viable and has been extensively studied both industrially and educationally for fast pyrolysis. Although, it is true, that it is limited in particle size (1–2 mm) and requires a large amount of inert gas, the great ability to transfer heat from the bed particles to the biomass makes this configuration optimal [19]. Recorded conversions to bio-oil in fluidized bed reactors are in the range of 60 to 80 wt.% of biomass on a dry basis under moderate operating conditions. Since the first pilot plants with very short residence times (less than 1 s) at the University of Waterloo in Canada, numerous projects have been developed [20]. It has also been very well received in studies to optimize pyrolysis parameters and pretreatments, such as with eucalyptus, where more than 60 wt.% conversion to bio-oil has been achieved and the amount of levoglucosan in it has been significantly improved by previous hydrothermal treatments [21]. Recent studies have developed projects to evaluate the characteristics of circulating fluidized reactors and the properties of the products obtained with typical lignocellulosic biomass such as sawdust and miscanthus [22]. Comparisons of different types of reactors in fast pyrolysis between auger, batch and fluidized bed have been carried out, and it has been concluded that a greater amount of bio-oil is obtained in a fluidized bed with properties very similar to the auger reactor [18]. Therefore, although there are numerous fast pyrolysis technologies, fluidized bed

reactors offer the best general guarantees of operation to obtain a high-quality bio-oil and, in addition, the flexibility can be applied to other thermochemical processes such as co-pyrolysis with domestic or industrial waste and gasification.

Pyrolysis is a complex process involving a large number of parameters, and when optimizing it is not sufficient to check these conditions one by one due to the immense number of runs required. However, the application of Response Surface Methods (RSM) to thermochemical treatments has proved to be effective in this type of situation. This statistical method has allowed researchers to successfully optimize by examining each individual parameter and the interactions that may occur between them, minimizing the number of experiments required and thereby saving costs [23]. It has been conveniently applied to the parameters of thermochemical treatments such as pyrolysis of torrefied biomass [24]. It has also been useful in evaluating the effects of temperature and particle size in the pyrolysis of biochar [25]. In particular, the optimization of the lignocellulosic biomass pyrolysis has focused on the reaction temperature, particle size and inert gas flow; but recently attempts have been made to introduce valuable parameters such as the condensation temperature of pyrolytic liquids or the introduction of some solid catalysts [26, 27]. Recent studies have aimed not only to maximize the yield of a given product, usually bio-oil, but also to improve its performance for its application in industry, since it is very common that it does not have the most suitable physicochemical properties (excess moisture, high content of oxygenated compounds, low stability) without previous treatments.

Lignocellulosic biomass pyrolysis in a fluidized bed reactor produces both high-quality bio-oil (compared to ASTM D7544-12 Standard Specification for Pyrolysis Liquid Biofuel) after condensation of the pyrolysis gases and by-products in the form of biochar and non-condensed gases together with the fluidization gas. The detailed analysis of the fractions once the process has been optimized is an important point to check the technological and economic feasibility of the technology. Gas chromatography/mass spectrometry is one of the most commonly used methods both to determine the compounds of both pyrolysis organic gases and bio-oil from previous extraction treatments with methanol, acetone or others [28, 29]. The characterization of non-condensed gases such as hydrogen, carbon monoxide, carbon dioxide and methane is usually performed by gas chromatography coupled to a conductivity detector, as in the case of pyrolysis studies of *Eichhornia crassipes* or catalytic pyrolysis of agricultural residues [30, 31]. As for the solid product or biochar, it is usually characterized as a typical solid fuel, very similar to traditional coal. The identification of parameters such as pH, thermal conductivity, calorific value and elemental composition, mainly based on C, H and O; are some of the most studied points. Some ratios (H/C and O/C) are widely used to determine the stability and properties of biochar in current applications, mainly as a soil amendment [32].

Experimentation with different technologies and species to determine the most favourable conditions continues to be a point to improve in thermochemical processes to lower costs and make them viable. Therefore, this study aims to optimize the pyrolysis of *L. leucocephala* in a pilot plant with a fluidized bed reactor, verifying the best guidelines to obtain a good yield of bio-oil, but also of non-condensed gas, biochar and quality of each one of the fractions, without sacrificing the economy of the process and the best pretreatment of the raw material. The optimization will allow recording the evolution of the fractions three-dimensionally for a better understanding of the process. In addition, the applications of each of the fractions (biochar, bio-oil and gas) will be evaluated in depth to produce sustainable biofuels and biochemicals. The production of renewable hydrogen through pyrolysis of *Leucaena leucocephala* is also addressed in this study as a potential producer of the energy vector.

Materials and methods

Raw material characterization

The samples of *L. leucocephala* have been obtained from a crop in "La Rábida" (Huelva, Spain) by the Agroforestry Group of the University of Huelva. The seeds of *L. leucocephala* originated in Australia. The raw harvested wood was stored, dried soon to a product with less than 10 wt.%, ground to a size between 1–5 cm and stored in bags in 2022. The wood chips are very heterogeneous and not suitable as feed for the pilot plant feeding. For this reason, the bags of *L. leucocephala* were removed and re-shredded using a Woodstock 3ph (Smartec, from Italy) to homogenize the wood into 0.7–1.5 mm chips. The wood samples used in the experiments were dried at 105 °C for 1 day. Part of the raw material was treated according to TAPPI T 249 cm–85 [33], standard method to obtain a chemical characterization of the *L. leucocephala* used in this study (extractives, acetyl groups, Klason lignin, glucan, xylan, arabinan, galactan, mannan). The ash content was obtained by subjecting the sample to 500 °C in a muffle. The results of the characterization are shown in Table 1 with bibliographical data for comparison [34, 35].

Pyrolysis/gasification system in pilot plant

A lab-scale fluidized bed reactor (PID Eng&Tech Micromeritics company), designed by the University of Huelva in collaboration with the Research Centre for Chemical Product and Process Technology (Pro^{2}TecS),

Table 1 Chemical composition of *L. leucocephala* from this study and other bibliographic compositions

	***L. leucocephala* (raw material)**		
	Present study	**Feria et al. [34]**	**Loaiza et al. [35]**
Ash (%)	1.7 ± 0.10	1.3	1.4
Extractives (%)	1.4 ± 0.06	1.1	–
Glucan (%)	36.4 ± 2.40	37.2	32.2
Klason lignin (%)	24.5 ± 1.80	22.4	21.5
Xylan (%)	16.2 ± 1.80	17.1	15.5
Arabinan (%)	0.1 ± 0.02	1.0	1.0
Galactan (%)	1.3 ± 0.30	–	–
Mannan (%)	1.1 ± 0.40	–	–
Acetyl groups (%)	1.7 ± 0.10	1.8	2.1

was used for the pyrolysis experiments (Fig. 1). The *L. leucocephala* pyrolysis system of this study is located in the teaching laboratories of the Higher Technical School of Engineering of Huelva (ETSI, Huelva, Spain).

The hopper is the first step in the pyrolysis process, the biomass is loaded prior to the start of the process and transported through an endless screw system into the reactor by a 2.25-cm-diameter steel tube. Shortly afterwards, the biomass is fed into the vertical fluidized bed reactor through a horizontal tube of 41.5 cm in length and 2.85 cm in diameter. The theoretical residence time of the solids in the reactor has been determined as the relationship between the fluid dynamic conditions of the gas injected at the bottom of the reactor and the thermodynamics of the sand bed inside. In this sense, to determine this theoretical residence time, both the balance of matter and the dynamics and thermodynamics of the fluids introduced and generated in the system have been calculated. Factors such a gas flow rate, velocity and particles characteristics have been taken into account in the fluid dynamics calculation [36]. The thermal energy required to complete the reaction is provided by a multi-zone electric heater, with three independent zones. Two ceramic fibres are installed in each zone to house the heating resistors. The temperature in each zone of the reactor is measured and controlled by three temperature sensors along the length of the reactor to ensure a uniform temperature throughout the reactor and to check that there is no axial temperature profile. The reactor is where the pyrolysis/gasification reaction takes place. It consists of a stainless-steel fluidized bed reactor with a maximum operating temperature of 850 °C at atmospheric pressure, divided into two zones: a reaction zone and a freeboard zone. The reaction zone is where the reactions take place, it is the lower part of the reactor (approximately 75.8 cm) and where the sand/catalyst is loaded and where it remains before being fluidized. There is a distribution plate inside the reactor to ensure that the bed remains in the same position. It is installed just below the feed inlet. Gases flow up through the distribution plate and fluidize the bed. The freeboard zone is located at the top zone of the reactor where the velocity of the gases is reduced to prevent a large amount of solids from leaving the reactor (approximately 128.2 mm). There is also a differential

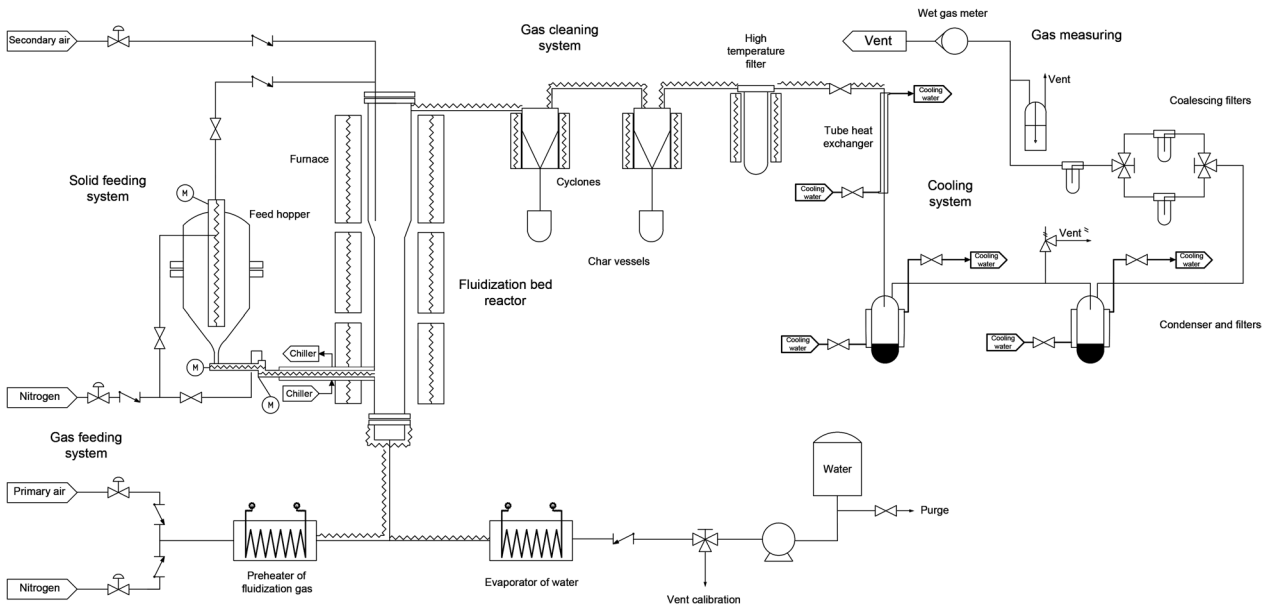

Fig. 1 Diagram of the pyrolysis/gasification pilot plant with fluidized bed reactor

pressure transmitter to measure the pressure drop across the length of the bed and two pressure transmitters to measure the pressure at the top and bottom of the reactor. Data were collected every second for each operating or maintenance period using the same software that controls the entire pilot plant called Process@ (V. 4.19.2.0., 07/09/2021, OPC SERVER license M85X40297).

The gas cleaning system is located at the outlet of the reactor and consists of two cyclones connected in series, which remove the char and ash present in the hot gases coming from the reactor and deposited in the storage vessels. Each cyclone is heated by an electrical resistance containing a thermocouple, and both an internal thermocouple. Finally, there is a 100-µm-high temperature filter to remove the smallest particles from the product gas stream that are not removed by the cyclones. Both cyclones, the filter and the process lines between them are heated to 450 °C to prevent the tar condensation.

The gas condensation system starts with a tubular heat exchanger to cool the hot gases and condense the tar and stream. The temperature at the outlet of the heat exchanger is controlled by a valve which regulates the inlet of the cooling fluid into the heat exchanger, in most cases water. Tar and water are collected in a cooling jacket vessel, the first condenser, at the bottom of the heat exchanger. Condensed liquids are retained, while the gas outlet goes to the second condenser to collect more tar and water. Finally, the product gases are sent to the coalescing filters. There are two manual three-way valves to direct the gases to the first or second filter. Once one of these filters is saturated, the operator must commutate the valves to direct the gases to the other filter. The amount of gas products produced during the process is measured by a wet gas meter. This wet gas meter is equipped with an absolute pressure transmitter and a thermocouple for direct normalization of the measured value. A check valve is installed upstream of this measured system to prevent overpressure within the instrument. In addition, the needle valve allows the user to take samples of the product gas before it enters in the wet gas meter.

The experimental design determined the specific conditions of each pyrolysis test. For each particular run, 500 g of *L. leucocephala* was pyrolyzed.

Statistical design

The experimental design for the optimization of the pyrolysis parameters of *L. leucocephala* was carried out using the SPSS (V. 27.0, USA) software, a data analysis and mathematical modelling program. The methodology used to select the experiments was the Box–Behnken design (BBD), an architecture based on a factorial design with three incomplete levels where each point is equidistant from a central point [37]. The number of experiments required for BBD is defined by $N = 2\ k \cdot (k-1) + C_0$, where N is the number of runs, k is the number of variables of interest, and C_0 is the number of desired central points [38]. In the fluidized bed pyrolysis of *L. leucocephala*, the following three variables have been selected: reaction temperature, nitrogen flow rate, and condensation temperature of the pyrolytic liquids in the first instance. All the values of the independent variables have been normalized to −1, 0 and 1, as shown in Table 2.

Table 2 Factors and levels used in the selected experimental design of *L. leucocephala* pyrolysis in the pilot plant

Factors	Variable	Level		
		−1	0	+1
Pyrolysis reaction temperature (°C)	*x*	400	500	600
Nitrogen flow rate (L/min)	*y*	2 Q_{mf}	3 Q_{mf}	4 Q_{mf}
Condensation temperature (°C)	*z*	70	90	110

For the reaction temperature, a factor widely studied in the bibliography, 400, 500 and 600 °C have been chosen. The nitrogen flow rate was varied between 2, 3 and 4 times the minimum fluidization flow rate (Q_{mf}), defined as the minimum gas flow that causes the force exerted by the bed particles to be equal to that of the ascending gas [39]. Most studies use fixed nitrogen flow rates (e.g., 4, 8 and 12 L min^{-1}) with response surface methods, but this approach, which takes into account bed hydrodynamics, is much more stringent to obtain suitable results. The condensing temperatures in the vertical heat exchanger were 70, 90 and 110 °C using domestic water at 20 °C as the refrigerant fluid. The total number of experiments was, therefore, 15, with 3 central points and 12 factorials. The conversion of leguminous biomass to biochar, bio-oil and non-condensed gas were studied as responses.

Characterization of pyrolysis products

Characterization of pyrolytic gases

Non-condensed gas samples were collected at the pilot plant outlet in fritted glass thermal desorption tubes (length: 88.9 mm; outer diameter: 6.35 mm, Supelco, Bellefonte, Pennsylvania, USA), by leaving a small valve open for 10 s and analysed according to Clemente-Castro et al. [40].

To evaluate the possible potential for hydrogen production by pyrolysis of *L. leucocephala*, a series of non-condensable gas samples have been collected. These samples were the result of experiments at three different reaction temperatures (400, 500 and 600 °C) in the reactor and were collected from pilot plant outlines. The gases, in 1 L Tedlar bags (Supelco, Bellefonte, Pennsylvania, USA)

until completely filled have been stored and analysed according to Palma et al. [41].

Bio-oil characterization

The volatile organic compounds in the liquid pyrolytic fraction have been determined by gas chromatography and mass spectrometry. First, samples of the obtained pyrolytic liquids under optimal operating conditions were freeze-dried at 0.6 mbar and − 50 °C in a Telstar Cryodos freeze-dryer (Telstar, Terrassa, Spain) for 2 days to remove all water from the bio-oil. After freeze-drying, the samples have been dried under nitrogen and 50 µL of both pyridine and BSTFA/TMCS (90:10) were added, followed by incubation for 30 min at 60 °C. The trimethylsilyl (TSM) derivative extracts has been diluted (1:25) with $CHCl_3$ and 1 µL was injected into a gas chromatogram–tandem mass spectrometry (GC–MS/MS) (GC–MS QP8030 Ultra System, Shimadzu, Tokyo, Japan). TMS-derived compounds were separated by a HP-5 MS (column length: 60 m, inner diameter: 0.25 mm, film thickness: 0.25 µm, J&W Scientific, Agilent Technologies, Santa Clara, California, USA). The GC oven was programmed as follows: 50 °C for 2 min, ramped at 8 °C min^{-1} to 280 °C, held for 2 min. A second ramp rate was performed at 50 °C min^{-1} to a final temperature of 300 °C, was reached and held for 2 min. Helium has been used as the carrier gas at a constant flow rate of 1.20 mL min^{-1}. The temperatures of the injection port (split mode 10:1), transfer line and ion source were maintained at 250, 280 and 230 °C, respectively. The mass spectrometer was operated in scan mode (50–800 m/z). TMS derivatives have been identified by comparison of the mass spectra with those in the NIST11 library database. GCMS Postrun Analysis Shimadzu was used for control and data analysis. The mass spectrometer was run on perfluorotributylamine (PFTBA).

A series of tests were carried out on the physicochemical properties of the bio-oil. The moisture content of the *L. leucocephala* raw material before entering the pyrolysis reactor was measured by heating it up to 105 °C for 2 h, in order to have references in terms for the quality of the obtained bio-oil. The Gross Calorific Value (GCV, constant volume) has been determined according to the standards "CEN/TS 14918:2005 (E) Solid Biofuels—Method for the determination of the calorific value" and UNE 164001 EX have been determined. An automatic isoperibol calorimeter Parr 6200 (Parr Instrument Company, Moline, Illinois, USA) has been used to determine the GCV. The percentage of water in the bio-oil was calculated using the Karl Fischer titration method (Karl-Fischer Titrators, Mettler-Toledo S.A.E., Barcelona, Spain). The solids content of the bio-oil obtained was determined using the D7579 method. This method describes a filtration procedure intended for all concentration ranges of pyrolysis solids. The viscosity of the pyrolysis liquid was measured using a DV2T model viscometer (Brookfield, USA). The density of the bio-oil, it was measured using the ASTM D1298 standard method. The sulphur content has been determined using an elemental analyzer (Eltra Helios C/H/S Analyzer autosampler, Haan, Germany). The ash content of the bio-oil has been measured according to ASTM D482 standard method. This test method covers the determination of ash in the range of 0.001–0.180% by mass of typical petroleum fuels. Finally, the acidity or alkalinity (pH) of the bio-oil has been determined using a pH meter (Crison pH meter Basic 20, Crison Instruments, Barcelona, Spain).

Solid fraction characterization

Several properties of interest were measured on the solid fraction obtained from the pyrolysis of *L. leucocephala* in the form of biochar at three reaction temperatures (400, 500 and 600 °C). For a better interpretation of the results, the properties listed below were also measured on the untreated raw material, with the exception of the pH value and the electrical conductivity. GCV according to the standards "CEN/TS 14918:2005 (E) Solid Biofuels—Method for the determination of the calorific value" and UNE 164001 EX have been determined. The GCV has been measured using a Parr 6200 Automatic Isoperibol Calorimeter (Parr Instrument Company, Moline, Illinois, USA). The distribution of carbon, hydrogen and sulphur in the biochar was simultaneously analysed using an elemental analyzer (Eltra Helios C/H/S Analyzer autosampler, Haan, Germany). The standard guidelines for the determination of carbon, hydrogen (EN 15104:2011) and sulphur (EN 15289:2011) have been followed. To determine moisture, volatile matter, fixed carbon, and ash content, a series of pyrolysis and combustion thermogravimetric analyses have been performed (Mettler Toledo thermogravimetry analyzer/DSC1 STARe system). In addition, the oxygen content by difference (CEN/TS 14961, 2005) has been also calculated taking into account the percentage of ash. A sample of biochar was air-dried and pulverized into fine particles (< 2 mm). Then, 1 g of the sample was weighed, and 20 mL of deionized water was added and manually shaken. The mixture was mechanically stirred at room temperature for 1 h (Gerstel twister stir plate, Mülheim an der Ruhr, Germany). The suspension was allowed to stabilize for 30 min. At this point, the suspension was collected, and the pH and electrical conductivity were measured using a pH meter (Crison pH meter Basic 20, Crison Instruments, Barcelona, Spain) and conductivity meter (Crison

EC meter GLP 31, Crison Instruments, Barcelona, Spain) [42].

Results and discussion

Analysis of response construction

To evaluate the evolution of the yields of the liquid phase ($\alpha_{bio\text{-}oil}$), non-condensed gas (α_{gas}) and, finally, biochar ($\alpha_{biochar}$), the effect of the reaction temperature in the pyrolysis reactor (x), the flow of nitrogen as fluidization gas (y) and the condensation temperature in the double-tube heat exchanger (z) were studied. The effect of temperature has already been studied on other occasions, but the fluidization flow taking as a reference values of minimum fluidization velocity has not been dealt with up to now, also adding the condensation temperature parameter evaluating the quality of the bio-oil obtained. The different variables have been interrelated to obtain a model of each reaction that best fitted the experimental results obtained.

The biochar yield ($\alpha_{biochar}$) was evaluated using a quadratic model to verify how the different parameters intervene in this response with significance at the 0.05 level. This response is not influenced by the most of the variables, but only depends on the conditions before the cyclone system, so the model must to be adjusted to the interesting variables of interest by reducing it. Once the model was reduced, it was significant with a value of $p < 0.0001$ and the expression for the biochar evolution can be observed in Eq. 1. As can be seen, the variable pyrolysis temperature (x) in the reactor stands out very much, well above the flow rate of nitrogen (y) used as fluidizing gas. The value of R^2 for the fitted model was 0.973, while the R^2 for the predicted value was 0.963 with a standard deviation of 4.402. These parameters suggest that the model is well adapted to the environment and accurately explains the response ($\alpha_{biochar}$):

$$\begin{aligned}\text{Biochar yield } (wt.\%) &= 11.7515 - -18.9100 \cdot x \\ &+ 2.9675 \cdot y + 33.7123 \cdot x^2 \\ &+ 4.6673 \cdot y^2 + 1.9450 \cdot x \cdot y.\end{aligned} \quad (1)$$

Regarding the conversion to bio-oil ($\alpha_{bio\text{-}oil}$), the most important and desired parameter in biomass pyrolysis processes, a quadratic model was fitted to observe the influence at 0.05 significance level. In this case, it was decided to also fit the model and reduce it as much as possible without affecting the response, because although all the variables studied are significant, there are some correlations between variables that have little effect on the response. The reduced model is shown in Eq. 2 and reflects a very high significance with a value of $p < 0.0001$. The pyrolysis temperature (x) is again the variable with the greatest influence, with the nitrogen flow (y) and the condensation temperature (z) influencing at a similar level, far from the first one. This model, with a greater number of variable conditions, is fitted at a very high level with an R^2 of 0.981 and for the fitted values with an R^2 of 0.966 with a standard deviation of 2.582, a high-quality model fit to the bio-oil response ($\alpha_{bio\text{-}oil}$):

$$\begin{aligned}\text{Liquid phase yield } (wt.\%) &= 50.5200 - 2.6913 \cdot x \\ &+ 3.6275 \cdot y - 3.7813 \cdot z \\ &- 25.5875 \cdot x^2 - 6.5200 \cdot y^2 \\ &- 1.0832 \cdot z^2 + 1.7350 \cdot x \cdot z.\end{aligned} \quad (2)$$

Finally, the non-condensed gas yield (α_{gas}) was evaluated using a quadratic model with a significance level of at least 0.05. This response also included all the variables, but not to the same extent as the pyrolytic liquids response, so the model was reduced to a less comprehensive expression. The reduced model for the conversion to non-condensed gas (α_{gas}) is shown in Eq. 3 and has a p-value < 0.0001. As can be seen, the pyrolysis temperature (x) is still the most predictive variable, followed by the nitrogen flow (y) and then the condensation temperature (z). The R^2 value for the reduced model was 0.982 with an R^2 for adjusted values of 0.964 and a standard deviation of 3.122. Therefore, the model was also of great significance for the non-condensed gas yield (α_{gas}):

$$\begin{aligned}\text{Gas phase yield } (wt.\%) &= 40.7100 + 19.4962 \cdot x \\ &- 6.5950 \cdot y + 2.0988 \cdot z \\ &- 8.4975 \cdot x^2 + 1.4800 \cdot y^2 \\ &+ 2.7975 \cdot z^2 - 2.3125 \cdot x \cdot y.\end{aligned} \quad (3)$$

In order to show some of the most representative experiments, Table 3 was constructed with the five most significant results from the 15 runs.

Two extreme points in the pyrolysis temperature (x) the most influential variable, and 3 experiments at 500 °C to observe the influence of the other variables have been selected. In addition, the values of the responses predicted by the model have been plotted alongside the model to observe its adaptation. As can be seen, at 400 °C a lot of solid is produced (61.35 wt.%) because the temperature is simply not high enough to react well with the biomass under these conditions, and at 600 °C a huge amount of gas is produced (55.24 wt.%), because too much is passed through, and it destroys the structure of the compounds formed into gas instead of remaining as compounds that can condense mainly through secondary reactions. Around 500 °C is the optimum where it has shown good conversions to bio-oil (50.25 wt.%), if the process works with more fluidization gas, as can be seen, more unreacted lignocellulosic biomass is produced, as we see there at 17.27 wt.% to biochar, and on the other

Table 3 Representative table of experimental and predicted values of pyrolysis of *L. leucocephala* in pilot plant with fluidized bed reactor

X-Pyrolysis temperature (°C)	Y-Nitrogen flow rate (L min^{-1})	Z-Cond. temperature (°C)	Experimental values			Predicted values		
			Biochar yield (wt.%)	Bio-oil yield (wt.%)	Non-condensed gas yield (wt.%)	Biochar yield (wt.%)	Bio-oil yield (wt.%)	Non-condensed gas yield (wt.%)
400	3 Q_{mf}	70	61.35	27.18	11.47	64.37	32.05	13.42
500	2 Q_{mf}	110	12.95	32.50	54.55	13.45	35.51	53.68
500	3 Q_{mf}	90	9.71	50.25	40.04	11.75	50.52	40.71
500	4 Q_{mf}	70	17.27	48.50	34.23	19.38	50.32	36.29
600	3 Q_{mf}	110	24.89	19.87	55.24	26.55	19.11	56.61

hand, if the fluidization flow rate is low, the time spent in the reactor it increases significantly, generating more non-condensed gas (54.55 wt.%). The influence of the condensation temperature can also be observed in these three runs at the centre point of the pyrolysis temperature, giving more bio-oil at a lower temperature in the double-tube condenser. Therefore, although the optimum bio-oil yield cannot be seen from these data alone, it can be intuited that it will be close to 500 °C, with about 3 or 4 times the minimum fluidization flow and clearly at a lower condensation temperature, will give us more bio-oil will, without taking into account the quality of this, since, it will certainly have a higher moisture content.

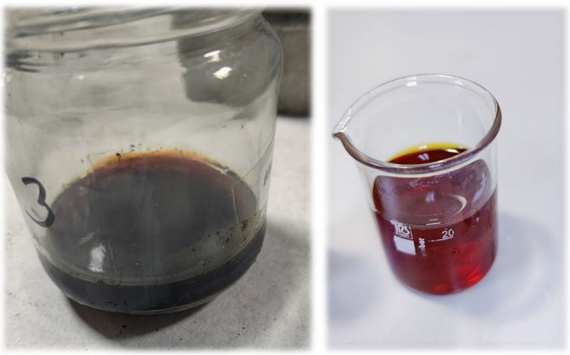

Fig. 2 Bio-oil collected by first and second condenser

Optimization of pyrolysis products

The most valuable parameter of the pyrolysis lignocellulosic biomass is the conversion into liquids, therefore it was the priority and the most valued product in the optimization of the study ($\alpha_{bio\text{-}oil}$). The maximum production of bio-oil in this fluidized bed reactor system occurs around 500 °C (x), 3.3 times the minimum fluidization flow (y), in this case, at 500 °C would be 26.4 L min^{-1} of pure nitrogen, and a condensation temperature of 70 °C (z). The moisture content of the bio-oil obtained was between 20 and 30 wt.%. in all the experiments at high condensation temperatures (90–110 °C), rising slightly to 30–35 wt.% for runs at 70 °C. As there are two condensers, it was possible to obtain good bio-oil conditions with a lower water content distributed between 82 and 89% in the first condenser and 11–18% in the second condenser (Fig. 2).

In the analysis of the fast pyrolysis products of *L. leucocephala*, the products were collected performing at 500 °C, 3 times the minimum fluidization flow (24 L min^{-1}), and 80 °C of condensation temperature, obtaining a high conversion to bio-oil (more than 50%) and a quality of the liquid.

In the case of biochar, this response surface is shown in Fig. 3a. In the case of biochar, the influence of the only two variables in this response, are the pyrolysis reaction temperature and the nitrogen flow, as the condensation temperature does not affect the system. As can be seen, there are two ranges of high conversion to solid: first, a large amount of biochar is produced at 400 °C, with peaks of up to 70% conversion and another at 600 °C, which produces less biochar but of higher quality (around 35% biochar yield). At low temperatures (400 °C), the reaction system simply does not have enough energy to degrade the fed lignocellulosic biomass and produces a lot of unreacted material that should not be called biochar. However, at high temperatures (600 °C), this solid fraction is the result of the breaking down of the complex lignin structures of the lignocellulosic biomass and is, therefore, of higher quality as a result of the complete degradation of the wood. At moderate temperatures (500 °C), there is a good conversion to bio-oil and gas, with suitable heat input, but without being too high to produce much gas and biochar. This is the minimum conversion to solids (around 10 wt.%). As the nitrogen flow rate increased, a curve with a tendency to increase in biochar formation was observed. The shorter the gas residence time in the pyrolysis reactor, the more unreacted

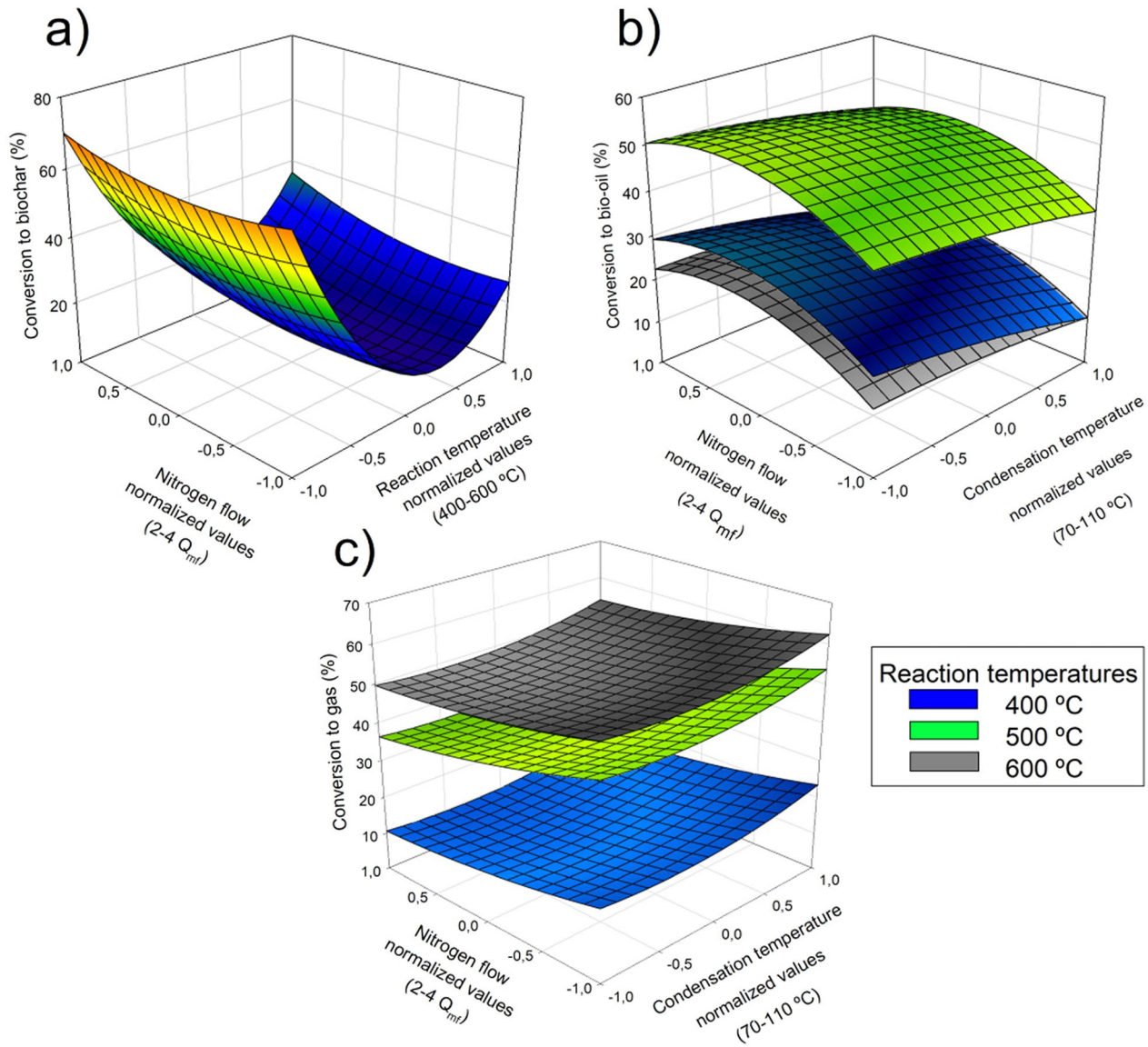

Fig. 3 Response surface plots of the different fractions of pyrolysis products of *L. leucocephala*. **a** Conversion to biochar, dependent on reaction temperature and nitrogen flow rate, **b** conversion to bio-oil, and **c** conversion to non-condensed gas

material is discharged. Although this effect is similar to that of temperature, it occurs to a much lesser extent, with a greater conversion to biochar, better termed unreacted material, at a higher nitrogen rate, as the biomass residence time is shorter. It is therefore, obvious that more solid is obtained at low temperature and high nitrogen flow rate, if a lot of unreacted material useful a solid fuel is desired, or at high temperature and high nitrogen flow rate, if a high-quality biochar with more specific applications to a large effective surface area is desired.

The trends in bio-oil conversion can be observed in Fig. 3b, where the variables nitrogen flow (y) and condensation temperature (z) are plotted at different reaction temperatures (x). The response surfaces, in this case, are three slightly concave planes, one of which is clearly superior for bio-oil production at 500 °C. The other two planes are much lower, although at 400 °C more bio-oil is obtained than at 600 °C, where the tendency is to form gas. The influence of the condensation temperature can be seen on its axis as a small curve where the best conversions to bio-oil are obtained at the low values. Significantly more bio-oil is produced at lower condensation temperatures, but at the cost of higher moisture content. When working with a condensation temperature

above 80–85 °C, good quality bio-oil with less than 30% moisture is obtained. The tendency to produce more non-condensed gas the higher the condensation temperature is evident, with this effect being much more pronounced at 400 °C in the pyrolysis temperature, where the organic compounds obtained are quite heavy and complex. This fact means that even the conversions to bio-oil at a condensation temperature of 110 °C are very similar in number to those at 400 and 600 °C, although the composition and formation of this liquid are diametrically different. Looking at the nitrogen flow rate, there is a curve with an upward trend, with more bio-oil being obtained at a higher flow rate because the residence time of the gases is shorter and secondary reactions that would produce more gas are prevented, this trend being consistent with the literature [43]. Although there is a tendency for more bio-oil to be produced at higher fluidization flow rates, this effect competes with the low residence time of the biomass in the reactor which causes less fluid to be formed, meaning that the optimum is not 4 times but rather less (3.3 times the minimum flow rate). This competition between reactions and residence times has been analysed and demonstrated in the literature, with models of the effects of conditions in bubbling reactors [44].

Finally, the gas yield curve shows a clear tendency for more gas to be formed at higher temperatures, as was to be expected, as shown in Fig. 3c. The optimum is the peak temperature (600 °C), a gas residence time as long as possible to improve the secondary reactions (2 Qmf) and a higher condensation temperature (110 °C) to avoid condensation as much as possible, as is well known. In this case, the highest amount of gaseous fraction was recorded with a value around of 55 wt.%, competing with the bio-oil, which still manages to condense, and the formation of more and more biochar from the lignin as the reaction temperature increases. These two trends, which have been extensively studied in the literature, are clearly observed in the three gas conversion response surfaces. Various studies have already detailed these effects at the pyrolysis reaction temperature where the gas increases as it grows [45] and how the gas flow reduces the residence time of the gases and, therefore, reduces the conversion to gas in favour of liquids [46].

Analysis of the pyrolysis products of L. leucocephala

Gas fraction

Volatile organic compounds in non-condensed gas The main volatile organic compounds (VOCs) detected in non-condensed gas at the outlet of the pilot plant are listed in Table 4.

These gases are accompanied by a large amount of nitrogen and other light non-condensed gases such as carbon dioxide, hydrogen, carbon monoxide or methane. The table shows only the 40 compounds that were detected in the highest proportions, as the amount of products in this process was very large due to the complex degradation of lignocellulosic structures. This gas stream is usually recirculated to the pyrolysis reactor as a fluidization gas in commercial pyrolysis reactors, although in some cases it is used as a fuel to improve the energy efficiency of the plant. In addition, there is increasing effort in the selective separation of compounds from this stream for specific applications, some of which will be discussed in the analysis of volatile organic compounds.

The detected compounds are mainly molecules derived from the degradation of hemicellulose and cellulose in the early stages of the chromatogram, and phenolic compounds derived from the degradation of lignin in the final stages. Some nitrogenous compounds were detected as ethyl 2-aminoethanimidate (1.92%) or pyridine (1.52%), together with aldehydes such as nona-2,6-dienal (0.89%) and other complex compounds such as 2,3-dihydro-1,4-dioxine (1.31%). Furans, typical of hemicellulose and cellulose degradation, were detected, in this case, as furfural (0.91%) and 2,5-dimethylfuran (2.52%). However, the most abundant compounds were ketones, simple aromatics, and phenols. About 12% were simple ketones such as 4-hydroxy-3-methylbutan-2-one (3.26%) or cyclic ketones, 2-hydroxy-3-methylcyclopent-2-en-1-one (2.07%). Large amounts of xylene (1.72%) and ethylbenzene (1.33%) were observed. There are academic efforts to produce renewable xylenes from improved lignocellulosic biomass pyrolysis are emerging, so this is an interesting product [47]. Not only were large amounts of methoxyphenols typical of lignin degradation are detected, but also a large amount of benzene polyols, which are simpler lignin degradation compounds that do not condense as well in the bio-oil. These aromatic compounds account for 18.57% (e.g., benzene-1,3-diol, 1.15%) while the more complex guaiacols and syringols represent 11.56% (e.g., 1,4-dimethoxy-2-methylbenzene, 1.26%). The anhydrosugars detected in this measurement was D-allose at 1.34%, a compound that has been observed in other analysis of *L. leucocephala* in thermochemical processes [40].

Analysis of permanent gases in non-condensed gas Using gas chromatography and thermal conductivity detector, it was possible to measure the concentration of hydrogen, carbon monoxide and carbon dioxide in the non-condensed gas obtained. From these concentrations, the conversion of each gas at different temperatures was calculated to assess its possible potential, the results of which are shown in Table 5.

Table 4 Organic compounds detected by gas chromatography/mass spectrometry in the non-condensed gas obtained from the pyrolysis of *L. leucocephala*

Compound	*L. leucocephala* Pilot plant, non-condensed gas (500 °C)			
	Formula	MW	RT (min)	Area (%)
Nona-2,6-dienal	$C_9H_{14}O$	138.21	4.020	0.89
Aldehydes				*0.89*
Ethyl 2-aminoethanimidate	$C_4H_{10}N_2O$	102.14	4.140	1.92
Pyridine	C_5H_5N	79.10	5.400	1.52
Nitrogen compounds				*3.44*
2,3-dihydro-1,4-dioxine	$C_4H_6O_2$	86.09	4.675	1.31
Dioxins				*1.31*
Furan-3-carbaldehyde	$C_5H_4O_2$	96.08	7.180	0.91
2,5-dimethylfuran	C_6H_8O	96.13	7.955	2.52
Furans				*3.42*
(E)-pent-3-en-2-one	C_5H_8O	84.12	5.240	1.94
4-Hydroxy-3-methylbutan-2-one	$C_5H_{10}O_2$	102.13	6.335	3.26
Cyclopentanone	C_5H_8O	84.12	6.495	1.38
2-Methylcyclopent-2-en-1-one	C_6H_8O	96.13	10.425	1.11
3-Methylcyclopent-2-en-1-one	C_6H_8O	96.13	12.370	0.89
2-Hydroxy-3-methylcyclopent-2-en-1-one	$C_6H_8O_2$	112.13	14.345	2.07
Ketones				*10.66*
1-Propoxybutane	$C_7H_{16}O$	116.20	5.840	2.12
2-Oxopropyl acetate	$C_5H_8O_3$	116.11	9.060	1.77
1-Propoxyheptane	$C_{10}H_{22}O$	158.22	25.825	1.12
Ethers				*5.01*
Ethylbenzene	C_8H_{10}	106.16	8.945	1.33
1,4-Xylene	C_8H_{10}	106.16	9.210	1.72
Phenol	C_6H_6O	94.11	12.840	1.96
2-Methylphenol	C_7H_8O	108.14	15.000	1.08
3-Methylphenol	C_7H_8O	108.14	15.580	2.17
2,4-Dimethylphenol	$C_8H_{10}O$	122.16	17.350	0.95
Benzene-1,2-diol	$C_6H_6O_2$	110.11	18.510	1.41
4-Methylbenzene-1,2-diol	$C_7H_8O_2$	124.14	19.820	1.46
Benzene-1,3-diol	$C_6H_6O_2$	110.11	20.140	1.15
4-Prop-2-enylphenol	$C_9H_{10}O$	134.17	20.245	1.09
4-(Hydroxymethyl)phenol	$C_7H_8O_2$	124.14	20.430	2.64
2,5-Dimethylbenzene-1,4-diol	$C_8H_{10}O_2$	138.16	21.610	0.91
2,3-Dimethylbenzene-1,4-diol	$C_8H_{10}O_2$	138.16	22.170	1.78
Aromatic compounds				*18.57*
2-Methoxyphenol	$C_7H_8O_2$	124.14	15.995	1.37
2-Methoxy-4-methylphenol	$C_8H_{10}O_2$	138.16	18.435	0.78
(3-Hydroxyphenyl) acetate	$C_8H_8O_3$	152.15	19.285	1.22
1-(4-Hydroxy-2-methylphenyl)ethanone	$C_9H_{10}O_2$	150.17	20.940	0.84
2-Methoxy-4-prop-2-enylphenol	$C_{10}H_{12}O_2$	164.20	21.740	0.85
4-Hydroxy-2-methoxybenzaldehyde	$C_8H_8O_3$	152.15	22.605	0.81
2-Hydroxy-5-methylbenzene-1,3-dicarbaldehyde	$C_9H_8O_3$	164.16	23.155	1.60
1,4-Dimethoxy-2-methylbenzene	$C_9H_{12}O_2$	152.19	23.240	1.26
2,3-Dimethylbenzoic acid	$C_9H_{10}O_2$	150.17	25.245	1.74
Lignin-derived compounds				*11.56*
2-Methylhexan-3-yl acetate	$C_9H_{18}O_2$	158.24	25.090	2.32
Butan-2-yl (E)-but-2-enoate	$C_8H_{14}O_2$	142.20	28.645	0.54

Table 4 (continued)

Compound	*L. leucocephala* Pilot plant, non-condensed gas (500 °C)			
	Formula	MW	RT (min)	Area (%)
Carboxylic acids				*2.86*
D-Allose	$C_6H_{12}O_6$	180.16	24.900	1.34
Anhydrosugars				*1.34*

Table 5 H_2, CO, CO_2 and CH_4 yields for the pyrolysis of *L. leucocephala* at the three temperatures studied

Temperature	Yield (wt. %)			
	H_2	CO	CO_2	CH_4
400 °C	0	1.05	4.74	0.78
500 °C	0.71	4.32	10.93	1.71
600 °C	1.54	7.89	11.75	2.06

At 400 °C, zero conversion to hydrogen was readily observed, indicating that at this stage of pyrolysis the energy is nowhere near sufficient to break the simplest C–H bonds. Although low, carbon monoxide (1.05 wt.%) and a higher conversion to carbon dioxide (4.74 wt.%) have been detected as a result of the degradation of simple hemicellulose and cellulose molecules. When the optimum point for bio-oil production at 500 °C have been reached, some changes were observed. Hydrogen started to be detected at a very low conversion (0.71 wt.%) and carbon monoxide also increased significantly (4.32 wt.%). In this case, although the aim was to obtain liquids, the system also obtained a large amount of non-condensed gas, so compounds such as carbon dioxide increased (10.93 wt.%). The energy was already sufficient to break difficult C–C and C–H bonds, so there was a first phase of very light detection of hydrogen and carbon monoxide. Analysing the data obtained at 600 °C, the point at which most non-condensed gas is obtained, there is a conversion to hydrogen of 1.54 wt.%. Carbon monoxide has also increased its conversion (7.89 wt.%), whereas carbon dioxide has hardly changed (11.75 wt.%) [48]. This indicates that the thermodynamics of the system changes towards an equilibrium where carbon monoxide predominates over carbon dioxide with increasing temperature. This distribution of the permanent gases obtained from lignocellulosic biomass pyrolysis has already been observed in recent studies on syngas production [49]. However, although this change increases the amount of hydrogen formed, it is still insufficient for the production of an industrial synthesis gas ($CO+H_2$), due to the low hydrogen content and the difficulty of separating nitrogen, at least not for processing this legume below 600 °C. As for methane, its conversion gradually increases with increasing temperature, stabilizing around 2 wt.% conversion by weight. Methane is formed by demethylation of secondary tar such as toluene into benzene and methane [50].

Liquid fraction

Physical and chemical analysis of the liquid fraction The bio-oil obtained from the fast pyrolysis of *L. leucocephala* is realistically valued on the market by comparison with the Standard Specification for Pyrolysis Liquid Biofuel ASTM D7544-12. These standard values and some bibliographic data on biomass pyrolysis in a fluidized bed reactor are shown in Table 6. In addition, some parameters of the fluidized bed reactor fast pyrolysis system of each study are shown. One of these parameters is the solids residence time, which was calculated as a mean based on the quotient between the fluidized bed height in metres and the fluid surface velocity in metres per second, at 600 °C of temperature and micronized biomass, obtaining an average residence time of 3.5 s. The residence time of the solids is controlled by the injected gas flow, which can be controlled by software.

The biomass particle size was kept between 0.2 and 1 mm in all cases. These ranges are justified because a smaller size of the material more does not imply a better bio-oil yield, because decreasing diameter of the biomass particles, the Reynolds number of the particles decreases and it becomes more difficult for biomass particles to be blown out of the reactor, reducing the residence time too much and causing more conversion to unreacted material [44]. Both the pyrolysis temperature and the condensation and feeding requirements were different in each system with its peculiarities, therefore, the results are only indicative. The calorific value obtained from the bio-oil calorimetry was very similar to that reported by Chanathaworn and Yatongchai [51] for *L. leucocephala* (18.87 and 19.60 MJ kg^{-1}, respectively), and since they are the same species, this provides a good guarantee of processing and it is concluded that the use of TiO_2 catalyst does not excessively improve the heat of combustion of the bio-oil. Other values are more dependent on the raw material and operating conditions. While lower values have been observed for other wood species, such as

Table 6 Properties physical and chemical of bio-oil of *L. leucocephala* pyrolysis in fluidized bed and other examples of bibliography

Characteristic	ASTM standard		Bio-oil *L. leucocephala*	Energy crops, *L. leucocephala*	Rice husk	Saccharina japonica	Pine sawdust	Waste furniture sawdust
	Grade G	Grade D	Own study	Chanathaworn and Yatongchai [51]	Li et al. [52]	Kim et al. [53]	Chen et al. [54]	Heo et al. [45]
Biomass particle size, mm	–	–	0.7–1.5	< 1	0.3–0.9	0.3–0.5	0.2–0.6	0.7
Biomass moisture content, wt.%	–	–	3.8	4.5	3.1	6.9	< 4	< 1
Temperature pyrolysis, °C	–	–	500	500 (TiO_2)	500	350	500	450
Solids residence time, s	–	–	3.5	–	–	–	–	–
Condensation system, °C	–	–	3 steps: 90–20–20	–	3 steps: 300–80–20	–20	4 steps: 20	–25
Nitrogen flow, L min^{-1}	–	–	24	–	330	18	60	5
Feed rate, kg h^{-1}	–	–	1	–	5	0.1	3	0.15
Gross heat combustion, MJ kg^{-1}	> 15	> 15	18.87	19.60	16.30	24.8	14.9	–
Water content, wt.%	< 30	< 30,0	27.35	8.1	–	–	33.21	45.2
Solids content, wt.%	< 2.5	< 0.25	–	0.24	–	–	–	–
Viscosity, mm^2 s^{-1} (40 °C)	< 125	< 125	13.56	11.42	5.57	–	9.1	–
Density at 20 °C, kg L^{-1}	1.1–1.3	1.1–1.3	1.22	1.2	1.06	–	–	–
Sulphur content, wt.%	< 0.05	< 0.05	0.04	0.015	–	–	–	–
Ash content, wt.%	< 0.25	< 0.15	0.12	0.98	–	–	–	–
pH	–	–	2.67	4.2	2.58	4.68	2.66	–
Flash point, °C	> 45	> 45	–	–	88	–	–	–
Pour point, °C	< –9	< –9	–	–	94	–	–	–

pine sawdust (14.9 MJ kg^{-1}) or rice husks (16.3 MJ kg^{-1}), the value for bio-oil from algae, *Saccharina japonica*, was significantly higher (24.8 MJ kg^{-1}) [52–54]. Regarding the moisture content of the bio-oil, in our study it was 27.35 wt.%, a rather high value, although it is still valid even for a grade D biofuel. In this case, the improvement of the process using a TiO_2 catalyst resulted in a great improvement of the water content of the bio-oil (8.1 wt.%), but this does not usually happen in pyrolysis processes of other woods such as furniture wood shavings or pine, where the moisture content is usually high (> 30%) [45, 51, 54]. All the other physical properties are favourable for *L. leucocephala* bio-oil, such as a correct density between 1.1 and 1.3 kg L^{-1} (1.22 kg L^{-1}), reduced viscosity (13.56 mm^2 s^{-1}), low ash and sulphur content (0.12 wt.% and 0.04 wt.%, respectively) and a not excessively low pH (2.67). The values of the *L. leucocephala* bio-oil from the bibliographic study are much higher in aspects such as moisture and moderate pH (4.2), this is because they used a TiO_2 catalyst to improve the efficiency of the process [51]. Therefore, although the bio-oil obtained meets the quality criteria for use as a Grade D biofuel in some parameters, reducing the amount of moisture is a priority in future studies to improve the stability of the liquid.

This liquid product can be used in many applications directly or as a power carrier after upgrading [55]. Bio-oil obtained by fast pyrolysis contains oxygenated organic compounds and water, which makes it unstable and corrosive. Therefore, it is necessary to improve

Table 7 Organic compounds detected by gas chromatography/mass spectrometry in the bio-oil obtained from the pyrolysis of *L. leucocephala*

Compound	*L. leucocephala* Pilot plant, bio-oil (500 °C)			
	Formula	MW	RT (min)	Area (%)
Butanedial	$C_4H_6O_2$	86.09	10.860	3.32
Butanal	C_5H_8O	72.11	14.437	1.47
Aldehydes				*4.79*
4-methylpyridine	C_6H_7N	93.13	12.565	0.84
2-[(2-amino-4-methylpentanoyl)amino]acetic acid	$C_8H_{16}N_2O_3$	188.22	14.935	1.05
Nitrogen compounds				*1.89*
1,4-dioxan-2-ol	$C_4H_8O_3$	104.10	11.037	2.57
(3,4,4-Trimethyldioxetan-3-yl)methanol	$C_6H_{12}O_3$	132.16	15.148	2.16
Dioxins				*4.73*
2H-Furan-5-one	$C_4H_4O_2$	84.07	16.890	3.03
3-Methyl-2H-furan-5-one	$C_5H_6O_2$	98.10	21.319	1.19
3-Methylfuran-2-carboxylic acid	$C_6H_6O_3$	126.11	27.600	0.68
Furans				*4.90*
(E)-But-2-enoic acid	C_4H_6O2	86.09	17.539	0.97
4-Ethoxybutanoic acid	$C_6H_{12}O_3$	132.16	27.315	1.13
Carboxylic acids				*2.10*
But-1-en-2-ol	C_4H_8O	72.11	11.858	1.58
3-Hydroxybutan-2-one	$C_4H_8O_2$	88.11	22.297	0.83
Ketones				*2.41*
1-({1-[(1-Methoxy-2-propanyl)oxy]-2-propanyl}oxy)-2-propanol	$C_{10}H_{22}O_4$	206.28	12.027	0.92
2-Ethoxyethanol	$C_4H_{10}O_2$	90.12	13.054	3.10
Ethane-1,2-diol	$C_2H_6O_2$	62.07	19.439	1.62
1-Ethoxypropan-2-ol	$C_5H_{12}O_2$	104.15	24.034	0.98
6-metHoxyhexan-2-ol	$C_7H_{16}O_2$	132.20	24.100	2.04
3,6,9,12-Tetraoxatetradecan-1,14-diol	$C_{10}H_{22}O_6$	238.23	25.027	1.83
Dodecaethylene glycol	$C_{24}H_{50}O_{13}$	546.60	26.937	1.61
1-Ethoxypropan-2-ol	$C_5H_{12}O_2$	104.15	27.518	1.10
Ether alcohols				*13.20*
2-(2-Oxocyclopent-3-en-1-yl)acetaldehyde	$C_7H_8O_2$	124.14	13.356	2.25
3-Methylcyclopent-2-en-1-one	C_6H_8O	96.13	18.720	3.22
(2S)-2-Hydroxypropanoic acid	$C_3H_6O_3$	90.08	19.836	0.85
2-Cyclopenten-1-one,2-hydroxy-3-methyl	$C_6H_8O_2$	112.13	20.780	1.67
3-Methylcyclopentane-1,2-dione	$C_6H_8O_2$	112.13	20.875	2.02
3-Ethyl-2-hydroxycyclopent-2-en-1-one	$C_7H_{10}O_2$	126.15	23.360	0.91
Cyclic ketones				*10.92*
Phenol	C_6H_6O	94.11	21.510	2.21
3-Methylphenol	C_7H_8O	108.14	22.077	2.57
Benzene-1,2-diol	$C_6H_6O_2$	110.11	25.290	1.67
4-Methylbenzene-1,2-diol	$C_7H_8O_2$	124.14	26.546	1.73
1,3-Benzenediol-2-methyl	$C_7H_8O_2$	124.14	27.150	1.48
Benzene-1,3-diol	$C_6H_6O_2$	110.11	28.183	1.76
1-Phenylethanol	$C_8H_{10}O$	122.16	28.645	1.01
4-Ethylbenzene-1,2-diol	$C_8H_{10}O_2$	138.16	28.962	1.88
4-Ethenylphenol	C_8H_8O	120.15	29.037	1.11
Aromatic compounds				*15.42*
4-Methoxyphenol	$C_7H_8O_2$	124.14	22.578	2.38
2-Methoxy-4-methylphenol	$C_8H_{10}O_2$	138.16	25.123	1.15

Table 7 (continued)

Compound	*L. leucocephala* Pilot plant, bio-oil (500 °C)			
	Formula	MW	RT (min)	Area (%)
2-Methoxybenzene-1,4-diol	$C_7H_8O_3$	140.14	26.724	1.83
2-Hydroxy-2-phenylacetic acid	$C_8H_8O_3$	152.15	27.095	1.34
2,6-Dimethoxyphenol	$C_8H_{10}O_3$	154.16	28.427	1.94
1-(3-Methoxy-4-propan-2-yloxyphenyl)propan-2-one	$C_{13}H_{18}O_3$	222.28	31.759	1.07
Lignin-derived compounds				*9.71*
(1R,2S,3S,4R,5R)-6,8-dioxabicyclo[3.2.1]octane-2,3,4-triol	$C_6H_{10}O_5$	150.17	25.643	1.25
Anhydrosugars				*1.25*

Table 8 Elemental analysis of biochar from *L. leucocephala* and examples from the literature [63–66]

Materials	Pyrolysis Temp. (°C)	C (%)	H (%)	S (%)	O (%)	N (%)	H/C	O/C
L. leucocephala	Raw material	47.3	6.1	0.10	41.6	–	0.13	0.88
Biochar 400	400 °C	51.7	2.6	0.55	32.6	–	0.05	0.63
Biochar 500	500 °C	63.4	3.1	063	19.0	–	0.05	0.30
Biochar 600	600 °C	57.4	1.8	0.46	16.3	–	0.03	0.28
Hardwood sawdust	500 °C	69.5	3.1	0.01	13.1	–	0.04	0.19
Wood waste	550 °C	91.4	2.8	0.00	4.6	–	0.03	0.05
Pine wood chip	465 °C	75.0	3.4	0.10	9.0	–	0.05	0.12
Beech	Raw material	49.1	5.7	–	44.7	–	0.12	0.91
Beech char 500	500 °C	64.9	4.3	–	28.2	–	0.07	0.43
Beech char 600	600 °C	76.7	2.7	–	15.9	–	0.04	0.21
Beech char 800	800 °C	77.4	2.7	–	14.3	–	0.03	0.18
Pine	Raw material	51.3	6.4	0.06	42.2	0.11	0.12	0.82
400 char pine	400 °C	76.8	3.3	0.21	19.1	0.57	0.04	0.25
600 char pine	600 °C	94.4	2.1	0.01	3.2	0.30	0.02	0.03
1000 char pine	1000 °C	97.3	0.4	0.01	1.2	1.15	0.00	0.01
Bamboo char	–	69.0	1.6	0.11	3.9	0.41	0.02	0.06
Rice husk char	–	42.7	2.4	0.15	2.4	0.51	0.06	0.06

deoxygenation to make it compatible with refinery fuels by hydrogenation normally [56]. Furthermore, it has been found that bio-oil contains many valuable components, such as phenols, aldehydes, and furans, which have the potential to be used for chemicals, such as resorcinol formaldehyde (RF) resin in particular [57]. Other recent studies show that fast pyrolysis bio-oil can be used to condition the soil. Bio-oil readily reacts with ammonia or urea to form organic nitrogen makes these compounds polymerize and solidify with heat to produce stable products called slow release fertilizers [58].

Gas chromatography–mass spectrometry bio-oil analysis The bio-oil obtained under optimal conditions for its maximum conversion was analysed by gas chromatography coupled to a mass spectrometer and the compounds obtained are shown in Table 7.

As in the case of non-condensed gas, the number of compounds detected was very high and it was necessary to select the 40 most abundant organic compounds, which represent about 70% of the total concentration.

In the liquid fraction, three types of organic compounds stand out above the rest: alcohols, ketones and phenols; all their molecules simple, complex or combinations between them. The chains of ether alcohols represent 13.20% of the total compounds between them, 2-ethoxyethanol (3.10%) or 6-methoxyhexan-2-ol (2.04%), and some glycols (ethylene glycol, 1.62% or dodecaethylene glycol, 1.61%). Minor compounds such as 4-methylpyridine (0.84%), an amino acid (2-[(2-amino-4-methylpentanoyl)amino]acetic acid, 1.05%), dioxins (e.g., 1,4-dioxan-2-ol, 2.57%), aldehydes (e.g., butanedial, 3.32%) and carboxylic acids ((E)-but-2-enoic acid, 0.97%) have been detected. Furans, which is well known

Table 9 Proximate analysis and physicochemical characteristics of biochar from *L. leucocephala* and examples from the literature [63–66]

Materials	Pyrolysis Temp. (°C)	Moisture (%)	Ash (%)	Volatile matter (%)	Fixed carbon (%)	pH	EC (μS cm^{-1})	HHV (MJ kg^{-1})
L. leucocephala	Raw material	3.60	1.70	82.30	16.10	–	–	19.17
Biochar 400	400 °C	3.10	12.59	44.45	39.86	8.64	1237	20.93
Biochar 500	500 °C	4.00	14.09	28.93	52.99	9.67	3.66	23.14
Biochar 600	600 °C	2.41	24.41	14.03	59.15	10.26	4.87	22.91
Hardwood sawdust	500 °C	–	–	–	–	–	–	–
Wood waste	550 °C	–	–	–	–	–	–	–
Pine wood chip	465 °C	–	–	–	–	–	–	–
Beech	Raw material	–	–	–	–	–	–	–
Beech char 500	500 °C	–	–	–	–	–	–	–
Beech char 600	600 °C	–	–	–	–	–	–	–
Beech char 800	800 °C	–	–	–	–	–	–	–
Pine	Raw material	5.63	0.76	79.25	14.36	–	–	–
400 char pine	400 °C	3.23	2.06	29.37	65.34	–	–	–
600 char pine	600 °C	2.81	2.62	11.83	82.74	–	–	–
1000 char pine	1000 °C	1.97	3.88	3.26	90.89	–	–	–
Bamboo char	–	21.60	25.00	11.70	41.70	–	–	24.99
Rice husk char	–	5.00	42.90	19.80	32.30	–	–	15.82

to be compounds of hemicellulose and cellulose degradation, were obtained in 4.90%, mainly 2H-furan-5-one (3.03%). A group of ketones in cyclic rings of five members accounted for 8.67% of the total, some of which were 3-methylcyclopent-2-en-1-one (3.22%) and 3-methylcyclopentane-1,2-dione (2.02%). Finally, there are compounds derived from lignin (25.13%), phenols that can be divided into two groups in the chromatogram studied: simple phenols and methoxyphenols. Simple phenols do not have methoxy bonds and were detected in 15.42%, they are mainly phenol (2.21%), diols (e.g., benzene-1,3-diol, 1.76%) and phenols with simple carbon chains (4-ethylbenzene-1,2-diol, 1.88%). The methoxy phenols (9.71%) are typical units of guaiacol and syringol, some are simple molecules such as 4-methoxyphenol (2.38%) and others are complex structures, such as 1-(3-methoxy-4-propan-2-yloxyphenyl)propan-2-one (1.07%). Before concluding this section, it is necessary to mention the presence of a very small proportion of levoglucosan (1.25%), the only anhydrosugar detected. Levoglucosan is the main component of cellulose degradation and is therefore an indicator of the amount of cellulose in the pyrolysis process of lignocellulosic biomass and, consequently, an indicator of bio-oil quality [29, 59].

Solid fraction

The amounts of biochar obtained at 400, 500 and 600 °C were 66.7 ± 3.2 wt.%, 11.9 ± 6.1 wt.% and 28.7 ± 1.4 wt.%, respectively. The solid conversions were slightly higher than those found by Ghorbel et al. [60], who showed a 31% yield of biochar from farm breeding compost at 300, 400 and 500 °C, and similar to the yields obtained from lignocellulosic biomass pyrolysis (25–40%) at the highest reaction temperature [61, 62]. The elemental composition and proximate analysis of the resulting biochar are shown in Tables 8, 9.

Moreover, the ash content of the resulting biochars increased significantly with respect to the feedstock ash due to the loss of organic matter to the gas phase during the pyrolysis process. Similarly, the carbon content of the biochar increased by 16.1% compared to the original legume biomass. The progressive concentration of carbon and minerals during volatilization caused by increasing temperatures can cause this process.

The H/C and O/C ratios to estimate the stability of biochar in soil are commonly used. According to Spokas [67], the O/C ratio could be a suitable indicator of biochar stability. In addition, according to Shakya and Agarwal [68], the O/C ratio can also inform us about the general polarity of the material. The polarity and abundance of polar oxygen-containing surface functional groups in biochar can be indicated by the O/C ratio [69]. Therefore, high values indicate higher polarity of functional groups. On the other hand, low O/C ratios, due to the adsorption mechanism shifts from being mainly based on ion exchange to physisorption [70], low adsorption capacity,

due to the weaker nature of physisorption, may indicate. In this study, high O/C ratios > 0.6 (0.9–1.0) have been found. These data may be indicative of a product that is not very stable in soil and therefore a low stability of the biochar produced can be assumed.

Also, the H/C ratio can be used as an indicator of the aromaticity and stability of biochar [71, 72]. Low values for this parameter have been found, therefore a low aromaticity can be shown.

These data, for different biomasses, are presented in Table 8 and Fig. 4.

Differences, mainly in the O/C ratio, with respect to other biochar have been found. The point corresponding to the solid obtained at 400 °C has an O/C ratio that is too high compared to typical biochar. This is due to the fact that at such a low temperature the reactor did not provide enough energy to decompose all the volatiles, resulting in high conversions to solid or unreacted wood, instead of biochar. Regarding the biochar obtained at 500 °C and 600 °C, both show a similar O/C ratio, although higher than that of typical biochars in the literature, so it can be said that the *L. leucocephala* biochar is stable but less than other biochars. The H/C ratio of the three solid products obtained hardly varies (0.051, 0.049 and 0.032, for 400, 500 and 600 °C), except for the one with the highest temperature, where a more pronounced decrease in the hydrogen concentration was observed, resulting in a biochar with lower aromaticity.

Moderate values of gross heating, 19.17, 23.14 and 22.91 MJ kg^{-1} for 400, 500 and 600 °C, respectively, have been found. The value obtained at 600 °C should be higher as it contains more carbon, but the high ash concentration in the material has caused a reduction. Values similar to 25–30 MJ kg^{-1} in biochars from different feedstocks have been found [73, 74], but higher than those found by Mierzwa-Hersztek et al. [75], in the range of 11–12 MJ kg^{-1} for sawdust, wheat straw, and miscanthus straw. In this regard, Tripathi et al. [76] showed that the calorific value of biochar is directly proportional to the process temperature and inversely proportional to the H/C and O/C molar ratios. The obtained data support the conclusions of these authors.

Alkalinity is one of the most influential properties of biochar, because changes in pH have a significant effect on many soil processes [77]. In this study, values of 8.64, 9.67 and 10.26 have been found for 400, 500 and 600 °C biochar, respectively. In this regard, Li et al. [78] and Fidel et al. [77] showed values between 5.5 and 10.3 depending on the biochar feedstock and pyrolysis conditions. The values found in biochar from *L. leucocephala*, are similar compared to those found by the previous authors, being slightly higher when the pyrolysis temperature and therefore its ash and salt content are increased. Observing the

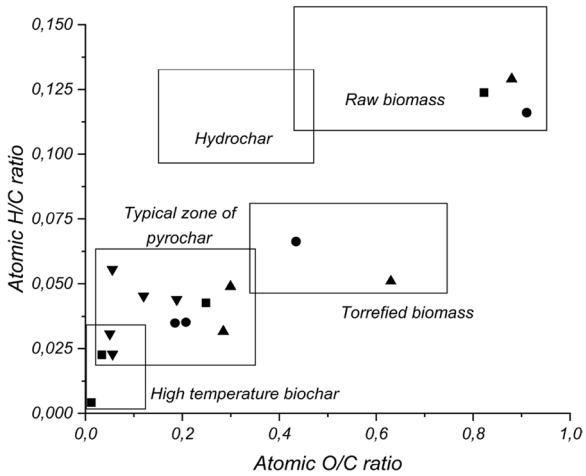

Fig. 4 Van Krevelen diagram of biochar and raw materials atomic H/C vs. O/C ratios (filled upward triangle *L. leucocephala* (own study), filled circle beech, filled square pine, filled downward triangle others bibliography biochar) [63–66]

electrical conductivity of the different biochar, it can be seen that in the case of biochar at 400 °C the conductivity is much higher (1237 μS cm^{-1}) than the other two biochar (3.66 and 4.87 μS cm^{-1}). This is another indication that the solid material obtained at 400 °C is not a product that can be called biochar, but an unreacted material very similar to roasted wood.

Conclusions

Fast pyrolysis can be used to obtain high-quality bio-oil, organic volatile non-condensed gas and biochar with different properties from lignocellulosic biomass, such as *L. leucocephala*. The behaviour of the product yield showed slight influence of both, nitrogen flow and temperature condensation, although the pyrolysis reaction temperature had a large influence on the product distribution.

At the intermediate temperature of 500 °C, a high liquid yield is obtained, which results in a high solid fraction at 400 °C and a high gas yield at 600 °C. Lower temperature of liquid condensation produces more bio-oil, however, as moisture increases, the optimum is determined to be around 80 °C or higher to give bio-oil with less than 30% of water content. Increasing the nitrogen flow rate results in greater bio-oil conversion up to about 3.3 times the minimum fluidization rate, obtaining bio-oil conversions around 55 wt.% with respect to raw material at optimum conditions.

Fast pyrolysis of *L. leucocephala* produces there valuable fractions: solid biochar, which can be obtained at 400 °C, giving a low-quality product with a large amount of unreacted material, or at 600 °C, a highly porous and valuable material; liquid, better called bio-oil, obtained

with reasonable yields at 500 °C and high nitrogen flow rates, a highly valued liquid in the industry as a biofuel and chemical precursor; and finally, a gaseous fraction, which can be burned for energy recovery, although more specific applications are rather limited due to its low organic content, low conversion to green hydrogen and high dilution in nitrogen as fluidizing gas.

Acknowledgements
All authors are members of the Research Centre for Chemical Products and Processes Technology (Pro2TecS).The authors acknowledge the contributions of other members of the Research Centre who contributed to thisstudy.

Author contributions
SCC: investigation, writing—review and editing, data analysis, validation. AP: conceptualization, investigation, methodology, writing—original draft, data analysis, visualization. MRM: conceptualization, investigation, methodology, supervision. IG: methodology, resources, data analysis, formal analysis. MJD: conceptualization, writing—review and editing, supervision, project administration, funding acquisition. All authors have read and agreed to the published version of the manuscript.

Funding
This study was supported by the Ministry of Economy and Competitiveness (Spain), as well as by the National Research Program Oriented to the Challenges of Society (Project PID2020-112875RB-C21 funded by MCIN/AEI/10.13039/501100011033), and the CEPSA Foundation Chair.

Availability of data and materials
The datasets used and analysed during the current study are available from the corresponding author upon reasonable request.

Declarations

Ethics approval and consent to participate
Not applicable.

Consent for publication
The authors consent to publishing the manuscript in *Environmental Sciences Europe*.

Competing interests
The authors declare that they have no competing interests.

Received: 3 August 2023 Accepted: 21 October 2023
Published online: 31 October 2023

References

1. Fahmy TYA, Fahmy Y, Mobarak F et al (2020) Biomass pyrolysis: past, present, and future. Environ Dev Sustain 22:17–32. https://doi.org/10.1007/s10668-018-0200-5
2. Alvarez-Chavez BJ, Godbout S, Palacios-Rios JH et al (2019) Physical, chemical, thermal and biological pre-treatment technologies in fast pyrolysis to maximize bio-oil quality: a critical review. Biomass Bioenerg 128:105333. https://doi.org/10.1016/j.biombioe.2019.105333
3. Czernik S, French R (2014) Distributed production of hydrogen by auto-thermal reforming of fast pyrolysis bio-oil. Int J Hydrogen Energy 39:744–750. https://doi.org/10.1016/j.ijhydene.2013.10.134
4. Treedet W, Suntivarakorn R (2018) Design and operation of a low cost bio-oil fast pyrolysis from sugarcane bagasse on circulating fluidized bed reactor in a pilot plant. Fuel Process Technol 179:17–31. https://doi.org/10.1016/j.fuproc.2018.06.006
5. Chen D, Zhou J, Zhang Q, Zhu X (2014) Evaluation methods and research progresses in bio-oil storage stability. Renew Sustain Energy Rev 40:69–79. https://doi.org/10.1016/j.rser.2014.07.159
6. Stedile T, Ender L, Meier HF et al (2015) Comparison between physical properties and chemical composition of bio-oils derived from lignocellulose and triglyceride sources. Renew Sustain Energy Rev 50:92–108. https://doi.org/10.1016/J.RSER.2015.04.080
7. Oasmaa A, Van De Beld B, Saari P et al (2015) Norms, standards, and legislation for fast pyrolysis bio-oils from lignocellulosic biomass. Energy Fuels 29:2471–2484. https://doi.org/10.1021/acs.energyfuels.5b00026
8. Ansari KB, Arora JS, Chew JW et al (2019) Fast pyrolysis of cellulose, hemicellulose, and lignin: effect of operating temperature on bio-oil yield and composition and insights into the intrinsic pyrolysis chemistry. Ind Eng Chem Res 58:15838–15852. https://doi.org/10.1021/acs.iecr.9b00920
9. Lédé J (2012) Cellulose pyrolysis kinetics: An historical review on the existence and role of intermediate active cellulose. J Anal Appl Pyrolysis 94:17–32. https://doi.org/10.1016/j.jaap.2011.12.019
10. Leng E, Guo Y, Chen J et al (2022) A comprehensive review on lignin pyrolysis: Mechanism, modeling and the effects of inherent metals in biomass. Fuel 309:122102. https://doi.org/10.1016/j.fuel.2021.122102
11. Naher UA, Choudhury ATMA, Biswas JC et al (2020) Prospects of using leguminous green manuring crop Sesbania rostrata for supplementing fertilizer nitrogen in rice production and control of environmental pollution. J Plant Nutr 43:285–296. https://doi.org/10.1080/01904167.2019.1672734
12. Aganda AA, Tshwenyane SO (2003) Lucerne, Lablab and Leucaena leucocephala Forages: Production and Utilization for Livestock Production. Pakistan J Nutr 2:46–53. https://doi.org/10.3923/pjn.2003.46.53
13. Fernández M, Alaejos J, Andivia E et al (2020) Short rotation coppice of leguminous tree *Leucaena* spp. improves soil fertility while producing high biomass yields in Mediterranean environment. Ind Crops Prod. https://doi.org/10.1016/j.indcrop.2020.112911
14. Basu P (2018) Biomass gasification, pyrolysis and torrefaction. Practical design and theory
15. Uddin MN, Techato K, Taweekun J et al (2018) An overview of recent developments in biomass pyrolysis technologies. Energies. https://doi.org/10.3390/en11113115
16. Aldaco R, Irabien A, Luis P (2005) Fluidized bed reactor for fluoride removal. Chem Eng J 107:113–117. https://doi.org/10.1016/j.cej.2004.12.017
17. Lakshman V, Brassard P, Hamelin L et al (2021) Pyrolysis of Miscanthus: Developing the mass balance of a biorefinery through experimental tests in an auger reactor. Bioresour Technol Reports. https://doi.org/10.1016/j.biteb.2021.100687
18. Nam H, Capareda SC, Ashwath N, Kongkasawan J (2015) Experimental investigation of pyrolysis of rice straw using bench-scale auger, batch and fluidized bed reactors. Energy 93:2384–2394. https://doi.org/10.1016/j.energy.2015.10.028
19. Qureshi KM, Kay Lup AN, Khan S et al (2021) Optimization of palm shell pyrolysis parameters in helical screw fluidized bed reactor: Effect of particle size, pyrolysis time and vapor residence time. Clean Eng Technol 4:100174. https://doi.org/10.1016/j.clet.2021.100174
20. Lappas AA, Samolada MC, Iatridis DK et al (2002) Biomass pyrolysis in a circulating fluid bed reactor for the production of fuels and chemicals. Fuel 81:2087–2095. https://doi.org/10.1016/S0016-2361(02)00195-3
21. Chang S, Zhao Z, Zheng A et al (2013) Effect of hydrothermal pretreatment on properties of bio-oil produced from fast pyrolysis of eucalyptus wood in a fluidized bed reactor. Bioresour Technol 138:321–328. https://doi.org/10.1016/j.biortech.2013.03.170
22. Park JY, Kim JK, Oh CH et al (2019) Production of bio-oil from fast pyrolysis of biomass using a pilot-scale circulating fluidized bed reactor and its characterization. J Environ Manage 234:138–144. https://doi.org/10.1016/j.jenvman.2018.12.104
23. Wu P, Zhang X, Wang J et al (2021) Pyrolysis of aquatic fern and macroalgae biomass into bio-oil: comparison and optimization of operational parameters using response surface methodology. J Energy Inst 97:194–202. https://doi.org/10.1016/j.joei.2021.04.010
24. Singh S, Chakraborty JP, Mondal MK (2020) Pyrolysis of torrefied biomass: optimization of process parameters using response surface methodology, characterization, and comparison of properties of pyrolysis oil from raw biomass. J Clean Prod 272:122517. https://doi.org/10.1016/j.jclepro.2020.122517
25. El Hanandeh A, Albalasmeh A, Gharaibeh M (2021) Effect of pyrolysis temperature and biomass particle size on the heating value of biocoal

and optimization using response surface methodology. Biomass Bioenerg 151:106163. https://doi.org/10.1016/j.biombioe.2021.106163
26. Álvarez-Chávez BJ, Godbout S, Le Roux É et al (2019) Bio-oil yield and quality enhancement through fast pyrolysis and fractional condensation concepts. Biofuel Res J 6:1054–1064. https://doi.org/10.18331/BRJ2019.6.4.2
27. Ly HV, Park JW, Kim SS et al (2020) Catalytic pyrolysis of bamboo in a bubbling fluidized-bed reactor with two different catalysts: HZSM-5 and red mud for upgrading bio-oil. Renew Energy 149:1434–1445. https://doi.org/10.1016/j.renene.2019.10.141
28. Park JW, Heo J, Ly HV et al (2019) Fast pyrolysis of acid-washed oil palm empty fruit bunch for bio-oil production in a bubbling fluidized-bed reactor. Energy 179:517–527. https://doi.org/10.1016/j.energy.2019.04.211
29. Trubetskaya A, von Berg L, Johnson R et al (2023) Production and characterization of bio-oil from fluidized bed pyrolysis of olive stones, pinewood, and torrefied feedstock. J Anal Appl Pyrolysis 169:105841. https://doi.org/10.1016/j.jaap.2022.105841
30. Akubo K, Nahil MA, Williams PT (2019) Pyrolysis-catalytic steam reforming of agricultural biomass wastes and biomass components for production of hydrogen/syngas. J Energy Inst 92:1987–1996. https://doi.org/10.1016/J.JOEI.2018.10.013
31. Tran TK, Kim N, Leu HJ et al (2021) The production of hydrogen gas from modified water hyacinth (Eichhornia Crassipes) biomass through pyrolysis process. Int J Hydrogen Energy 46:13976–13984. https://doi.org/10.1016/j.ijhydene.2020.08.225
32. Klasson KT (2017) Biochar characterization and a method for estimating biochar quality from proximate analysis results. Biomass Bioenerg 96:50–58. https://doi.org/10.1016/j.biombioe.2016.10.011
33. TAPPI T 249 cm-85 (1985) Carbohydrate composition of extractive-free wood and wood pulp by Gas-Liquid Chromatography. In TAPPI Test Methods, Atlanta, G.A: Technical Association of the Pulp and Paper Industry.
34. Feria MJ, López F, García JC et al (2011) Valorization of Leucaena leucocephala for energy and chemicals from autohydrolysis. Biomass Bioenerg 35:2224–2233. https://doi.org/10.1016/j.biombioe.2011.02.038
35. Loaiza JM, López F, García MT et al (2017) Biomass valorization by using a sequence of acid hydrolysis and pyrolysis processes. Applicat Leucaena leucocephala Fuel 203:393–402. https://doi.org/10.1016/j.fuel.2017.04.135
36. Bruchmüller J, van Wachem BGM, Gu S et al (2012) Modeling the thermochemical degradation of biomass inside a fast pyrolysis fluidized bed reactor. AIChE J 58:3030–3042. https://doi.org/10.1002/AIC.13705
37. Ferreira SLC, Bruns RE, Ferreira HS et al (2007) Box-Behnken design: an alternative for the optimization of analytical methods. Anal Chim Acta 597:179–186. https://doi.org/10.1016/j.aca.2007.07.011
38. Kalantzi S, Kekos D, Mamma D (2019) Bioscouring of cotton fabrics by multienzyme combinations: application of Box-Behnken design and desirability function. Cellulose 26:2771–2790. https://doi.org/10.1007/s10570-019-02272-9
39. Anantharaman A, Cocco RA, Chew JW (2018) Evaluation of correlations for minimum fluidization velocity (Umf) in gas-solid fluidization. Powder Technol 323:454–485. https://doi.org/10.1016/j.powtec.2017.10.016
40. Clemente-Castro S, Palma A, Ruiz-Montoya M et al (2022) Pyrolysis kinetic, thermodynamic and product analysis of different leguminous biomasses by Kissinger-Akahira-Sunose and pyrolysis-gas chromatography-mass spectrometry. J Anal Appl Pyrolysis. https://doi.org/10.1016/j.jaap.2022.105457
41. Palma A, Doña-Grimaldi VM, Ruiz-Montoya M et al (2020) MSW compost valorization by pyrolysis: influence of composting process parameters. ACS Omega 5:20810–20816. https://doi.org/10.1021/acsomega.0c01866
42. Singh B, Dolk MM, Shen Q, Camps-Arbestain M (2017) Biochar pH, electrical conductivity and liming potential. Biochar A Guid to Anal Methods 23–38
43. Montoya JI, Valdés C, Chejne F et al (2015) Bio-oil production from Colombian bagasse by fast pyrolysis in a fluidized bed: an experimental study. J Anal Appl Pyrolysis 112:379–387. https://doi.org/10.1016/j.jaap.2014.11.007
44. Xiong Q, Aramideh S, Kong SC (2013) Modeling effects of operating conditions on biomass fast pyrolysis in bubbling fluidized bed reactors. Energy Fuels 27:5948–5956. https://doi.org/10.1021/ef4012966
45. Heo HS, Park HJ, Park YK et al (2010) Bio-oil production from fast pyrolysis of waste furniture sawdust in a fluidized bed. Bioresour Technol 101:S91–S96. https://doi.org/10.1016/j.biortech.2009.06.003
46. Kim JY, Oh S, Hwang H et al (2014) Assessment of miscanthus biomass (Miscanthus sacchariflorus) for conversion and utilization of bio-oil by fluidized bed type fast pyrolysis. Energy 76:284–291. https://doi.org/10.1016/j.energy.2014.08.010
47. He Y, Zhu L, Luo Y et al (2021) Selective upgrading of biomass pyrolysis oil into renewable p-xylene with multifunctional M/SiO2/HZSM-5 catalyst. Fuel Process Technol 213:106674. https://doi.org/10.1016/j.fuproc.2020.106674
48. Zhou N, Zhou J, Dai L et al (2020) Syngas production from biomass pyrolysis in a continuous microwave assisted pyrolysis system. Bioresour Technol 314:123756. https://doi.org/10.1016/j.biortech.2020.123756
49. Chuayboon S, Thermodynamic SA, Solar-El (2021) Metallurgical Zn Production To cite this version : HAL Id : hal-03221078
50. Dufour A, Masson E, Girods P et al (2011) Evolution of aromatic tar composition in relation to methane and ethylene from biomass pyrolysis-gasification. Energy Fuels 25:4182–4189. https://doi.org/10.1021/ef200846g
51. Chanathaworn J, Yatongchai C (2022) Upgrading of bio-oil from energy crops via fast pyrolysis using nanocatalyst in a bubbling fluidized bed reactor. Int Energy J 22:71–80
52. Li P, Shi X, Wang X et al (2021) Bio-oil from biomass fast pyrolysis: Yields, related properties and energy consumption analysis of the pyrolysis system. J Clean Prod 328:129613. https://doi.org/10.1016/j.jclepro.2021.129613
53. Kim SS, Ly HV, Choi GH et al (2012) Pyrolysis characteristics and kinetics of the alga Saccharina japonica. Bioresour Technol 123:445–451. https://doi.org/10.1016/j.biortech.2012.07.097
54. Chen T, Deng C, Liu R (2010) Effect of selective condensation on the characterization of bio-oil from pine sawdust fast pyrolysis using a fluidized-bed reactor. Energy Fuels 24:6616–6623. https://doi.org/10.1021/ef1011963
55. Czernik S, Bridgwater AV (2004) Overview of applications of biomass fast pyrolysis oil. Energy Fuels 18:590–598. https://doi.org/10.1021/EF034067U
56. Sorunmu Y, Billen P, Spatari S (2020) A review of thermochemical upgrading of pyrolysis bio-oil: techno-economic analysis, life cycle assessment, and technology readiness. GCB Bioenergy 12:4–18. https://doi.org/10.1111/GCBB.12658
57. Ren X, Cai H, Du H, Chang J (2017) The preparation and characterization of pyrolysis bio-oil-resorcinol-aldehyde resin cold-set adhesives for wood construction. Polym 232(9):232. https://doi.org/10.3390/POLYM9060232
58. Fernandez-Akarregi AR, Makibar J, Cueva F, et al (2010) High Quality Fertilizers Based on Biomass Pyrolysis Bio-oil and Char. In: Proc. 18th Eur. Biomass Conf. Exhib. pp 961–966
59. Hakeem IG, Halder P, Marzbali MH et al (2021) Research progress on levoglucosan production via pyrolysis of lignocellulosic biomass and its effective recovery from bio-oil. J Environ Chem Eng 9:105614. https://doi.org/10.1016/J.JECE.2021.105614
60. Ghorbel L, Rouissi T, Brar SK et al (2015) Value-added performance of processed cardboard and farm breeding compost by pyrolysis. Waste Manag 38:164–173. https://doi.org/10.1016/J.WASMAN.2015.01.009
61. Ghodake GS, Shinde SK, Kadam AA et al (2021) Review on biomass feedstocks, pyrolysis mechanism and physicochemical properties of biochar: State-of-the-art framework to speed up vision of circular bioeconomy. J Clean Prod 297:126645. https://doi.org/10.1016/J.JCLEPRO.2021.126645
62. Nurhadi N, Rianda S, Irawan C, Pramono GP (2021) Biochar production investigation from pyrolysis of lamtoro wood as a coal blend for fuel substitution in steam power plants. IOP Conf Ser Earth Environ Sci 749:012037. https://doi.org/10.1088/1755-1315/749/1/012037
63. Dang H, Wang G, Wang C et al (2021) Comprehensive study on the feasibility of pyrolysis biomass char applied to blast furnace injection and tuyere simulation combustion. ACS Omega 6:20166–20180. https://doi.org/10.1021/acsomega.1c01677
64. Fabbri D, Torri C, Spokas KA (2012) Analytical pyrolysis of synthetic chars derived from biomass with potential agronomic application (biochar). Relationships with impacts on microbial carbon dioxide production. J Anal Appl Pyrolysis 93:77–84. https://doi.org/10.1016/j.jaap.2011.09.012

65. Guizani C, Haddad K, Limousy L, Jeguirim M (2017) New insights on the structural evolution of biomass char upon pyrolysis as revealed by the Raman spectroscopy and elemental analysis. Carbon N Y 119:519–521. https://doi.org/10.1016/j.carbon.2017.04.078
66. Huang Y, Liu S, Akhtar MA et al (2020) Volatile–char interactions during biomass pyrolysis: understanding the potential origin of char activity. Bioresour Technol 316:123938. https://doi.org/10.1016/j.biortech.2020.123938
67. Spokas KA (2010) Review of the stability of biochar in soils: Predictability of O: C molar ratios. Carbon Manag 1:289–303. https://doi.org/10.4155/CMT.10.32/SUPPL_FILE/TCMT_A_10816161_SM0001.DOC
68. Shakya A, Agarwal T (2017) Poultry litter biochar: an approach towards poultry litter management–a review. Int J Curr Microbiol Appl Sci 6:2657–2668. https://doi.org/10.20546/IJCMAS.2017.610.314
69. Rangabhashiyam S, Balasubramanian P (2019) The potential of lignocellulosic biomass precursors for biochar production: Performance, mechanism and wastewater application—A review. Ind Crops Prod 128:405–423. https://doi.org/10.1016/J.INDCROP.2018.11.041
70. Ahmad M, Lee SS, Dou X et al (2012) Effects of pyrolysis temperature on soybean stover- and peanut shell-derived biochar properties and TCE adsorption in water. Bioresour Technol 118:536–544. https://doi.org/10.1016/J.BIORTECH.2012.05.042
71. Wei L, Huang Y, Huang L et al (2020) The ratio of H/C is a useful parameter to predict adsorption of the herbicide metolachlor to biochars. Environ Res 184:109324. https://doi.org/10.1016/J.ENVRES.2020.109324
72. Xiao X, Chen Z (2016) Chen B (2016) H/C atomic ratio as a smart linkage between pyrolytic temperatures, aromatic clusters and sorption properties of biochars derived from diverse precursory materials. Sci Reports 61(6):1–13. https://doi.org/10.1038/srep22644
73. Jiang KM, Cheng CG, Ran M et al (2018) Preparation of a biochar with a high calorific value from chestnut shells. New Carbon Mater 33:183–187. https://doi.org/10.1016/S1872-5805(18)60333-6
74. Tsai CH, Tsai WT, Liu SC, Lin YQ (2018) Thermochemical characterization of biochar from cocoa pod husk prepared at low pyrolysis temperature. Biomass Convers Biorefinery 8:237–243. https://doi.org/10.1007/S13399-017-0259-5/FIGURES/2
75. Mierzwa-Hersztek M, Gondek K, Jewiarz M, Dziedzic K (2019) Assessment of energy parameters of biomass and biochars, leachability of heavy metals and phytotoxicity of their ashes. J Mater Cycles Waste Manag 21:786–800. https://doi.org/10.1007/S10163-019-00832-6/FIGURES/5
76. Tripathi M, Sahu JN, Ganesan P (2016) Effect of process parameters on production of biochar from biomass waste through pyrolysis: a review. Renew Sustain Energy Rev 55:467–481. https://doi.org/10.1016/J.RSER.2015.10.122
77. Fidel RB, Laird DA, Thompson ML, Lawrinenko M (2017) Characterization and quantification of biochar alkalinity. Chemosphere 167:367–373. https://doi.org/10.1016/J.CHEMOSPHERE.2016.09.151
78. Li M, Liu Q, Guo L et al (2013) Cu(II) removal from aqueous solution by Spartina alterniflora derived biochar. Bioresour Technol 141:83–88. https://doi.org/10.1016/J.BIORTECH.2012.12.096

Publisher's Note